Automatic Water Body Extraction using Multispectral Thresholding

K.P. Sivagami*, S.K. Jayanthi

Abstract--- Industrialization and urbanization lead to change in land use patterns and increase in utilization of water resources. Timely monitoring of surface water and delivering data on the dynamics of surface water are essential for policy and decision making processes. Change detection based on multispectral and multi temporal remote sensing data is one of the most acceptable and ever growing surface water change detection mechanisms in recent years. In this paper, a study has been conducted to detect the water bodies present in Erode region of Tamil Nadu based on Resourcesat-2 LISS-III November 2011 data using Normalized Difference Water Index and Thresholding based techniques. The result illustrates the effectiveness of the Bi-level Bi-stage Multispectral Thresholding approach for identification of water bodies and hence applied to detect the changes in water bodies during the period of 2011 to 2014.

Keywords--- Bi-level Bi-Stage Multispectral Thresholding, Change Detection, Surface Water Body Extraction, Water Indices.

I. INTRODUCTION

Water bodies on the Earth's surface have been changed largely due to global climatic changes and increasing human activities. These changes affect the agricultural and industrial production as well as ecological and environmental security. Regional economic development and environmental protection needs the information about the spatial distribution and area of water bodies. Water mapping and change detection based on satellite remote sensing images have become a major approach in recent years due to the rapid development of remote sensing technology.

There exist two broad categories of water body extraction methods; one is the traditional supervised and unsupervised classification using a single band or multiple bands, and the other one is the water related spectral index and threshold based approaches. Generally, supervised classification technologies based on spectral signature analysis can effectively identify and detect large water bodies. The index and threshold based approaches have been widely used to identify water bodies, due to the unique spectral characteristics of water bodies in the visible and infrared bands (Yan Zhou et al. 2017).

The index and threshold based water body mapping approaches have undergone a succession of evolution. Hence, in this paper, the spectral absorption characteristic of water in the visible, Near Infrared (NIR) and Shortwave Infrared (SWIR) bands are used for multispectral thresholding and Normalized Difference Water Index (NDWI) to extract the water bodies from Resourcesat-2 Linear Imaging and Self Scanning Sensor (LISS-III) imagery.

The aim of this paper is to extract and quantify the level of water surface area present in Erode region and identify the changes that had undergone over the period 2011 to 2014 using remotely sensed Resourcesat imageries.

II. RELATED WORKS

Water bodies are the most precious resource in Earth, and they may change in time and space as a consequence of climate change, land cover change, and other environmental changes. For the last four decades, series of optical remote sensing sensors such as Resourcesat, Landsat, and Worldview etc. are continuously observing and capturing the earth surface. Different spatial, spectral, and temporal resolution data provided by the sensors are reliable information for the study of environmental changes with low cost. Hence, many researchers have been focused on detecting the change of land use / land cover as a whole or any particular interest such as farmland, forest, urban and water (Tri Dev et al. 2017).

Recently several image processing techniques have been introduced to extract the surface water bodies from satellite data based on spectral indices or multiband techniques. Many improved indices have been proposed to obtain better results in a particular environment, such as the normalized difference vegetation index (NDVI), NDWI, modified NDWI (mNDWI), Tasseled Cap Wetness Index (TCWI), Automated Water Extraction Index (AWEI) and Land Surface Water Index (LSWI) (Stuart 2013, Komeil et al. 2014, Yan Zhou et al. 2017).

The performances of different water body mapping algorithms have been examined by Yan Zhou et al. (2017) and identified the NDWI-based algorithms performed better than the algorithms based on other water indices.

Wenbo et al. (2013) recommended the indices using the green band and the SWIR band are the most efficient indices for detecting water body information in the Earth Observation-1 Advanced Land Imager data.

In this work, NDWI using green band and NIR band ($NDWI_{24}$) (Stuart 2013, Komeil et al. 2014, Shridhar and Alvarinho 2014, Amare 2016, Satya and Ashwani, 2016, Tri Dev et al. 2017, Yan Zhou et al. 2017), NDWI using green band and SWIR band ($NDWI_{25}$) (Wenbo et al. 2013), NIR band multi threshold (Otsu-NIR), and multispectral multi threshold (Otsu-SNR) methods have been implemented and identified the suitable method for surface water change detection.

Manuscript received February 01, 2019

K.P. Sivagami*, Associate Professor, Department of Computer Science, JKK Nataraja College of Arts and Science, Tamil Nadu, India. (e-mail: kpsivaravi@gmail.com)

S.K. Jayanthi, Associate Professor, Department of Computer Science, Vellalar College for Women, Tamil Nadu, India.

III. STUDY AREA AND DATA ACQUISITION

The Indian Remote Sensing (IRS) Resourcesat-2 LISS III Sensor data available from ISRO Bhuvan, a National Remote Sensing Centre (NRSC) Open Earth Observation data archive portal (bhuvan.nrsc.gov.in/data/), were used in this study. A geographical area bounded between latitude 11.25N to 11.5N and longitude 77.5E to 77.75E is selected as the study area which bounds several water bodies that are situated in and around Erode region, Tamil Nadu. The received data are ortho corrected and operates in three visible NIR spectral bands and

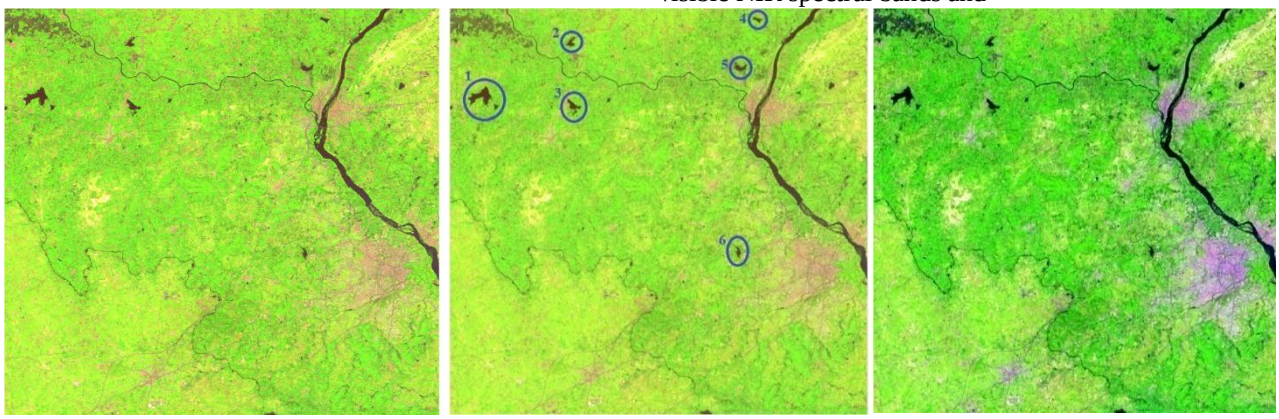

a Study area **b Sample Water Bodies** **c Enhanced Image**

Fig. 1: False Colour Composite - 543 bands (SWIR, NIR, Red) of Study area of Erode region (Resourcesat-2 LISS-III November, 2011)

one SWIR band with 24-metre spatial resolution, path-row number 100-065, tile name C43F11 and a swath of 141 km. The data acquired on 09 November 2011 (as reference data) and 17 November 2014 (as test data) have been used for this study to identify the changes occurred during 2011 to 2014 in the water bodies.

3.1 Colour Composite Images

For visual display, the multispectral images can be displayed by one band at a time as a gray scale image or combination of three bands at a time as a colour composite image since they consist of several bands of data. Colour composite images can be generated by associating each spectral band arbitrarily to a separate primary colour guns (red, green, and blue). In the true colour composite images, the colours of the resulting image have the resemblance of its actual colour. Rest of the resultant images are called as false colour composite images.

A very common false colour composite combination for displaying multispectral image is assigning the Red, Green, and Blue display guns with NIR, red and green bands (432 bands) respectively. Another common combination is assigning the Red, Green, and Blue display guns with SWIR, NIR, and red bands (543 bands). The study area used for this work in false colour composite is shown in Fig. 1.a.

The water bodies used for this study are 1. Odathurai Pond (WB-1), 2. Appakodal Lake (WB-2), 3. Ananda sagaram lake (WB-3), 4. Thalakulam Lake (WB-4), 5. Kadayampatti Lake (WB-5), and 6. Karuvilparai valasu kulam (WB-6) and the location map of Erode region with these water bodies is shown in Fig. 1.b.

Among the water bodies, WB-1 is large in area, whereas WB-4 and WB-6 are small and the rest are medium. The source of water for these lakes is from monsoon rain and fed by a canal from Bhavanisagar Dam under Lower-Bhavani-Project (LBP). The smaller lakes are surrounded by farmlands. All these water bodies serve for irrigation in the surrounding areas.

The ortho rectified input data are dull due to unbalanced colours and subtle contrast. Hence, they have been enhanced through de-correlation stretch followed by linear contrast stretch (Sivagami et al. 2017). The enhanced study area is shown in Fig. 1.c. The water features have been extracted individually from the temporal data to detect the area of water surface and analyze the changes.

IV. METHODOLOGY

Remote sensing is a reliable information source which provides synoptic coverage of fairly large areas at frequent intervals with low cost. Numerous algorithms have been implemented for mapping the spread of water bodies from satellite data (NRSC report 2014). Nowadays object oriented classification based on image segmentation has drawn more attention because the segmentation results determine the accuracy of classification through thresholding.

Among many threshold selection methods, Otsu is the optimum one in the sense that it maximizes the between-class variance, a well known measure used in statistical discriminant analysis. Based on Otsu threshold, the images were classified into two classes in two stages to differentiate the land-water boundary using Bi-level Bi-stage Multispectral Thresholding (Sivagami et al. 2016). In the spectral indexing process, the index value is generated by performing arithmetic operation on two spectral bands and the images were classified by the threshold of the index which is selected based on the spectral characteristics of the region of interest (Gulcan and Mehmet 2017). The performance of each satellite-derived index classifiers and Otsu based classifiers were compared with the reference maps which are generated manually using visual interpretation.

4.1 Spectral Water Indices

Water indices refer to mathematical models that enhance the water signals for a given pixel in the images obtained

Published By:
Blue Eyes Intelligence Engineering
& Sciences Publication

from visible, near-infrared and other scanning sensors. These models are usually calculated from green, near-infrared, mid-infrared and shortwave infrared portions of the spectrum (Amare 2016). The water index developed for the extraction of water features from Resourcesat-2 imageries is NDWI.

The NDWI was first proposed by McFeeters in 1996. The water shows the high percentage of reflectance in green band contrast to the near infrared and short infrared bands. These band combinations are used for the partition of water feature from other land features of the earth surface by using the appropriate threshold factor for the NDWI and the threshold for water is greater than zero (Gulcan and Mehmet 2017). The ratio of difference between green band and NIR band to the sum of these bands gives the $NDWI_{24}$ value.

$$NDWI_{24} = \frac{Green - NIR}{Green + NIR} \quad (4.1)$$

The water bodies $g(x, y)$ have been extracted by,

$g(x, y) = 1$ if $NDWI_{24}(x, y) > 0$ (4.2)
$= 0$ otherwise

The ratio of difference between green band and SWIR band to the sum of these bands gives the $NDWI_{25}$ value.

$$NDWI_{25} = \frac{Green - SWIR}{Green + SWIR} \quad (4.3)$$

The water bodies $g(x, y)$ have been extracted from $NDWI_{25}$ by,

$g(x, y) = 1$ if $NDWI_{25}(x, y) > 0$ (4.4)
$= 0$ otherwise

4.2 Bi-level Bi-stage Multispectral Thresholding

The most successful thresholding methods are based on histogram technique and the input image is in gray scale. The satellite images have multiple bands and the information is coded in each band. So when these images are converted into grayscale, there is a chance for information loss. To avoid such information loss multispectral perception has been introduced in the Bi-level Bi-stage Multispectral Thresholding (B^2MST) algorithms. This algorithm generates three threshold values (low, middle, and high) for each spectral band. The water body has been extracted using low threshold values in each spectral band (Sivagami et al. 2016).

4.2.1 Otsu-SNR Algorithm

In this algorithm, the water body has been extracted in two stages using Otsu threshold for SWIR, NIR, and Red bands. For each band, global threshold (mid) is calculated and the image is segmented into two classes in the first stage, and in the next stage, local threshold value is calculated for each class (low and high). Finally the water body $g(x, y)$ is extracted from the input image $f(x, y)$ of size $M \times N$ using low threshold values $SWIR_{low}$, NIR_{low}, and red_{low} of three bands SWIR, NIR, and red as,

$g(x, y) = 1$ if $((SWIR(x, y) < SWIR_{low})$ or $(Red(x, y) < Red_{low}))$ and $(NIR(x, y) < NIR_{low})$ (4.5)
$= 0$ otherwise

for $x = 0,1,2,...,M-1$ and $y = 0,1,2,...,N-1$. Finally the water surface area is calculated for each water bodies in terms of number of pixels.

4.2.2 Otsu-NIR Algorithm

The NIR band is strongly absorbed by water and is very much reflected by the terrestrial vegetation and dry soil (Komeil et al. 2014). Owing to this reason bi-level bi-stage Otsu threshold values NIR_{mid} and NIR_{low} were calculated for NIR band and the water bodies $g(x, y)$ have been extracted by,

$g(x, y) = 1$ if $(NIR(x, y) < NIR_{low})$ (4.6)
$= 0$ otherwise

where $NIR(x, y)$ is the NIR band of input image $f(x, y)$.

4.3 Performance Measures

In order to evaluate the effectiveness of the proposed approaches for the detection of surface water, the reference maps were generated carefully by on-screen digitizing of the water surface area in multi-temporal Resourcesat-2 LISS III 2011 image (false colour composite 543 bands) using visual interpretation. The classification accuracy of water extraction was evaluated by comparing the results of automatic water body extraction algorithms, Otsu-SNR, Otsu-NIR and the standard algorithms $NDWI_{24}$, $NDWI_{25}$ with reference data.

One of the most common means of expressing classification accuracy is the preparation of error matrix called confusion matrix. It compares the relationship between known reference data and the corresponding results of an automated classification on a category-by-category basis (Lillesand et al. 2004).

4.3.1 Overall Accuracy

The ratio between the sum of elements along the diagonal in the confusion matrix and the total number of reference pixels gives the overall accuracy of classification.

$$Overall\ Accuracy = \frac{Sum\ of\ Diagonal\ Elements}{Total\ number\ of\ Pixels} \quad (4.7)$$

4.3.2 Kappa Coefficient / KHAT Statistic

The overall statistical agreement of confusion matrix can be measured by Kappa coefficient which takes non-diagonal elements into account and computed as

$$\hat{k} = \frac{N\sum_{i=1}^{r} x_{ii} - \sum_{i=1}^{r}(x_{i+} \cdot x_{+i})}{N^2 - \sum_{i=1}^{r}(x_{i+} \cdot x_{+i})} \quad (4.8)$$

where

r = number of rows in the error matrix
x_{ii} = number of observations in row i and column i (on the major diagonal)
x_{i+} = total of observations in row i
x_{+i} = total of observations in column i
N = total number of observations included in matrix

The performance of $NDWI_{24}$, $NDWI_{25}$, Otsu-NIR and Otsu-SNR methods are evaluated for the water bodies in the year 2011 with reference data.

4.4 Change Detection

In order to detect the changes in the surface area of water bodies in Erode region for the period of 2011 to 2014 using the multi-temporal Resourcesat-2 LISS-3 Nov'11 (reference data) and Nov'14 (test data) images, the interested water

bodies were extracted individually in each temporal image. The total number of pixels present in each water body were calculated and compared with the reference data to identify the changes over the period of 2011 to 2014.

V. RESULTS AND DISCUSSION

Resourcesat-2 LISS-3 data were obtained for the region of Erode and preprocessing was performed to remove the dull appearance for visibility. The reference data generated manually from the preprocessed November 2011 RGB-543 false colour composite image and the results obtained by the standard and proposed methods are shown in Fig. 2.

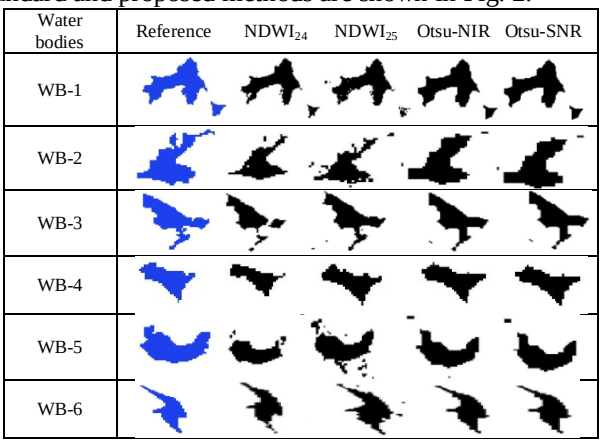

Fig. 2: Outcomes of all the methods for the study area with reference image

Reference datasets were selected from November 2011 data and the number of pixels in each water surface as a reference was calculated by cropping the water bodies manually. The results obtained by using $NDWI_{24}$, $NDWI_{25}$, Otsu-NIR and Otsu-SNR for the same image with reference data are listed in Table 1.

Table 1: Number of Pixels Identified in each water body

Water Body	Sample Size	Number of Pixels Identified as Water Surface				
		Reference	NDWI 24	NDWI 25	Otsu-all	Otsu-NIR
WB-1	111x131	1639	1306	1379	1555	1565
WB-2	81x81	389	223	257	374	397
WB-3	81x81	569	412	523	531	532
WB-4	81x81	225	133	202	213	227
WB-5	81x81	434	287	471	408	412
WB-6	81x81	277	184	358	221	221
Total	47346	3533	2545	3190	3302	3354

$NDWI_{24}$: Green and NIR band **Otsu-SNR**: SWIR, NIR, Red bands
$NDWI_{25}$: Green and SWIR band **Otsu-NIR**: NIR band **WB**: Water Body

5.1 Classification Error Matrix

Confusion matrices in Table 2 to Table 5 have been prepared to determine how well the water bodies are categorized by different methods using the known water body surface area (reference data) and the pixels actually identified as water body surface area in each samples by the classifier.

Table 2 NDWI24 - Green & NIR bands

Classes	BGD	WB-1	WB-2	WB-3	WB-4	WB-5	WB-6	R Tot
BGD	43807	1	1	0	0	0	4	43813
WB-1	334	1305	0	0	0	0	0	1639
WB-2	167	0	222	0	0	0	0	389
WB-3	157	0	0	412	0	0	0	569
WB-4	92	0	0	0	133	0	0	225
WB-5	147	0	0	0	0	287	0	434
WB-6	97	0	0	0	0	0	180	277
C Tot	44801	1306	223	412	133	287	184	47346

BGD: Others; **WB**: Water Body; **C Tot**: Column Total; **R Tot**: Row Total

From the non diagonal column elements of Table 2, almost negligible amount of pixels (6 pixels out of 43813 pixels) were improperly included (commission error) in the water body category. Since water has a strong absorption capacity of NIR band, other than water bodies have been avoided effectively by $NDWI_{24}$ method using Green and NIR bands. Conversely, considerable amount of pixels in the water bodies remain unclassified (omission error) have been identified from the nondiagonal row elements of Table 2.

Table 3: $NDWI_{25}$ - Green & SWIR bands

Classes	BGD	WB-1	WB-2	WB-3	WB-4	WB-5	WB-6	R Tot
BGD	43510	34	9	18	24	104	114	43813
WB-1	294	1345	0	0	0	0	0	1639
WB-2	141	0	248	0	0	0	0	389
WB-3	64	0	0	505	0	0	0	569
WB-4	47	0	0	0	178	0	0	225
WB-5	67	0	0	0	0	367	0	434
WB-6	33	0	0	0	0	0	244	277
C Tot	44156	1379	257	523	202	471	358	47346

BGD: Others; **WB**: Water Body; **C Tot**: Column Total; **R Tot**: Row Total

From the nondiagonal column elements of Table 3, it has been observed that $NDWI_{25}$ method with SWIR and green bands improperly includes other pixels in the water body category. Omission of water body pixels have also been observed from the nondiagonal row pixels.

Table 4: Otsu - NIR band

Classes	BGD	WB-1	WB-2	WB-3	WB-4	WB-5	WB-6	R Tot
BGD	43622	46	60	25	33	27	0	43813
WB-1	120	1519	0	0	0	0	0	1639
WB-2	52	0	337	0	0	0	0	389
WB-3	62	0	0	507	0	0	0	569
WB-4	31	0	0	0	194	0	0	225
WB-5	49	0	0	0	0	385	0	434
WB-6	56	0	0	0	0	0	221	277
C Tot	43992	1565	397	532	227	412	221	47346

BGD: Others; **WB**: Water Body; **C Tot**: Column Total; **R Tot**: Row Total

Similarly the error matrices of Otsu-NIR and Otsu-SNR method in Table 4 and Table 5 show the omission of water pixels and improper inclusion of other pixels as water body pixels. Minimum number of omission occurs in Otsu-SNR method compare to Otsu-NIR.

Table 5: Otsu-SNR - SWIR, NIR and Red bands

Classes	BGD	WB-1	WB-2	WB-3	WB-4	WB-5	WB-6	R Tot
BGD	43663	41	40	24	20	25	0	43813
WB-1	125	1514	0	0	0	0	0	1639
WB-2	55	0	334	0	0	0	0	389
WB-3	62	0	0	507	0	0	0	569
WB-4	32	0	0	0	193	0	0	225
WB-5	51	0	0	0	0	383	0	434
WB-6	56	0	0	0	0	0	221	277
C Tot	44044	1555	374	531	213	408	221	47346

BGD: Others; **WB**: Water Body; **C Tot**: Column Total; **R Tot**: Row Total

Comparison of omission and commission errors occurs in four methods for all water bodies are given in Table 6. Even though the $NDWI_{24}$ method gives highest performance in commission error, it produces worst performance in omission error.

Published By:
Blue Eyes Intelligence Engineering
& Sciences Publication

Table 6: Comparison of Omission and Commission errors

Errors	Methods	WB-1	WB-2	WB-3	WB-4	WB-5	WB-6	Total
Commission	$NDWI_{24}$	0	1	0	1	0	4	6
	$NDWI_{25}$	24	9	18	34	104	114	303
	Otsu-NIR	20	40	24	41	25	0	150
	Otsu-SNR	33	60	25	46	27	0	191
Omission	NDWI-24	92	167	157	334	147	97	994
	NDWI-25	47	141	64	294	67	33	646
	Otsu-NIR	32	55	62	125	51	56	381
	Otsu-SNR	31	52	62	120	49	56	370

WB: Water Bodies

From the Fig.3, it has been observed that the method $NDWI_{25}$ is the highest position in commission error and second highest position in omission error. The Otsu based methods take lowest two positions in both errors but in vice-versa.

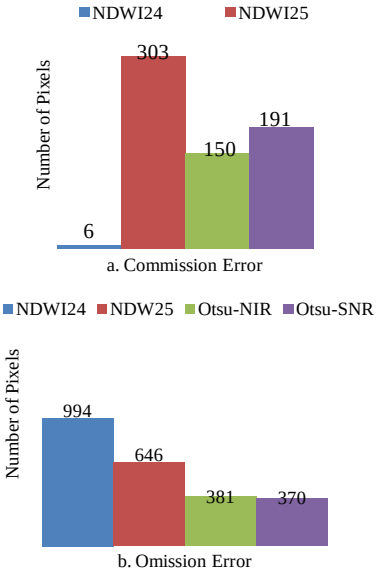

Fig. 3: Comparisons of Errors

Since the aim of this study is to identify the change detection in water bodies, both omission and commission errors should be minimum. Hence, the confusion matrices are subject to detailed interpretation and further analyzed statistically. The descriptive measures that can be obtained from the confusion matrix are overall accuracy and kappa coefficient (Lillesand et al. 2004).

Table 7: Measures for Water Bodies in Total

Measures (in %)	$NDWI_{24}$	$NDWI_{25}$	Otsu-NIR	Otsu-SNR
Overall Accuracy	97.89	98	98.82	**98.88**
Kappa	82.85	85.22	91.46	**91.85**

Overall accuracy incorporates the diagonal elements whereas the kappa measure incorporates the non diagonal elements of the error matrix as a product of the row and column marginal (Lilles and et al. 2004) and the results have been listed in Table 7.

From the chart in Fig.4, it has been noted that the overall accuracy and kappa coefficient of Otsu based methods are best compared to the standard index based methods. The highly reliable method associated with the water classification from Otsu based is Otsu-SNR.

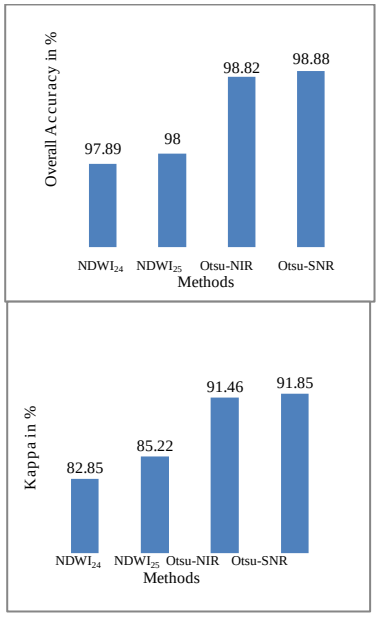

a. Overall Accuracy b. Kappa Coefficient

Fig. 4: Comparison of Performance

5.2 Change Detection

Once the required method has been identified, the change detection was performed by identifying water surface in November 2014 temporal image. The sample water bodies from November 2014 image of false colour composite 543-bands and their water surface detected by Otsu-SNR method are shown in Fig. 5 and Fig. 6.

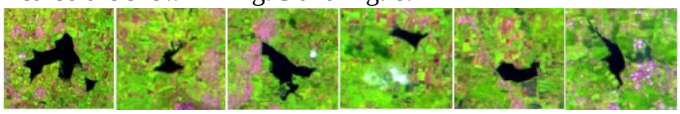

WB-1 WB-2 WB-3 WB-4 WB-5 WB-6

Fig. 5: Water Bodies of November 2014

WB-1 WB-2 WB-3 WB-4 WB-5 WB-6

Fig. 6: Extracted water bodies of November 2014

After extracting the water surface in each water body for the year 2014, the number of pixels extracted as water body has been calculated and listed in Table 8 along with reference data.

Table 8: Changes of Water Surface Area (in pixels)

Water Bodies	Surface Area			
	November 2011	November 2014		
	Reference	Estimated	Changes	% of Changes
WB -1	1555	1690	135	8.68
WB - 2	374	265	-109	-29.14
WB - 3	531	528	-3	-0.56
WB - 4	213	204	-9	-4.23
WB - 5	408	321	-87	-21.32
WB - 6	221	279	58	26.24

Comparison chart in Fig. 7 shows the changes in surface of water bodies for the two periods. From the figure, it has been clearly identified that in all water bodies there exist a very significant and discernible change occurs in its surface area cover.

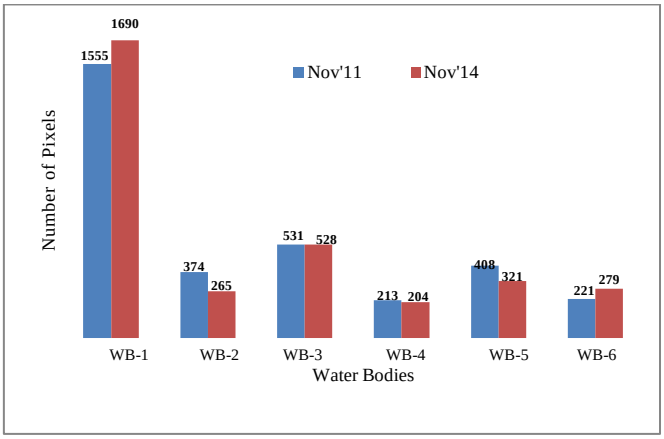

Fig. 7: Comparisons of Surface Water Bodies

The positive and negative changes in the surface of water bodies with respect to reference data for the years 2011 and 2014 in the same month have been shown in Table 8. A comparative analysis was performed to study the water surface changes in six water bodies of Erode region.

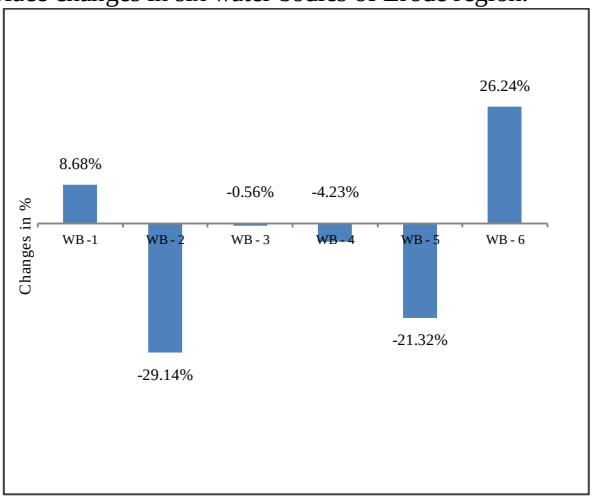

Fig. 8: Change Detection of Water Surface in Nov'14 with Respect to Nov'11

The results in Fig. 8, indicate that the surface of Odathurai pond and Karuvilparai valasu kulam are increased by 9% and 26% respectively. Maximum decrease occurs in Appakodal lake surface area by 30% compared to Nov'11 water surface. Similarly, Kadayampatti lake area also reduced to 21%. In the case of Ananda sagaram lake, the changes are almost nil (1%). There is a small reduction occurs in Thalakulam lake compared to reference value.

VI. CONCLUSION

Extracting the rivers, lakes and other inland water bodies from remotely sensed imagery is important for regular monitoring of water resources to evaluate the flood prediction, update the GIS database and long term climate model analysis (NRSC report 2014). The wide range of natural and manmade biological system has been supported by the surface water resources in India. The research of this article set an example for water identification method through multi thresholding in a small region of Tamil Nadu. The data is collected from Resourcesat-2 LISS-3 repository.

Water bodies from November 2011 image were extracted using proposed Otsu-NIR and Otsu-SNR methods and compared with standard algorithms $NDWI_{24}$ and $NDWI_{25}$. The fraction of pixels identified with each of these methods indicates that the automated algorithm provides better results compared to $NDWI_{24}$ and $NDWI_{25}$. The performance measures such as overall accuracy and kappa coefficient were used to analyze the outcome of these methods and concluded that Otsu-SNR provides better result. This algorithm was further applied on November 2014 image and the results were analyzed to identify the changes occurred in November month of 2011 and 2014. Seasonal changes can be easily evaluated using the proposed method. This work can be extended to different seasons in different years to study the temporal and seasonal changes of different regions.

REFERENCES

1. Amare Sisay, 'Remote sensing based water surface extraction and change detection in the Central Rift Valley Region of Ethiopia,' American Journal of Geographic Information System, 2016, 5(2), 33-39.
2. Geophysical products development division technical **report**, "Surface water layer products from OCM2 for BHUVAN NOEDA,' Geophysical and spectral products, SDAPSA, NRSC, September 2014 (available online: bhuvan.nrsc.gov.in/data/download/tools/.../ocm2_water_layer_BHUVAN_NOEDA.pdf).
3. Gulcan Sarp, Mehmet Ozcelik, 'Water body extraction and change detection using time series: A case study of Lake Burdur, Turkey,' ScienceDirect, Journal of Taibah University for Science, 2017, 11, 381-391 (open access: http://creativecommons.org/licenses/by-nc-nd/4.0/).
4. Himanshu Rana, Nirvair Neeru, 'Water Detection using Satellite Images Obtained through Remote Sensing,' Advances in Computational Sciences and Technology, 2017, 10(6), 1923-1940.
5. Komeil Rokni , Anuar Ahmad, Ali Selamat, Sharifeh Hazini, 'Water Feature Extraction and Change Detection Using Multitemporal Landsat Imagery,' Remote Sensing, 2014, 6, 4173-4189.
6. Lillesand, T.M., Kiefer, R.W., Chipman, J.W., 'Remote Sensing and Image Interpretation,' Fifth Edition, John Wiley & Sons (Asia) Pte. Ltd., Singapore, 2004; 586-593.
7. Satya Prakash Maurya, Ashwani Kumar Agnihotri, 'Evaluation of course change detection of Ramganga river using remote sensing and GIS, India,' Weather and Climate Extremes, 2016, 13, 68–72.
8. Shridhar D. Jawak, Alvarinho J. Luis, 'A Semiautomatic Extraction of Antarctic Lake Features Using Worldview-2 Imagery,' Photogrammetric Engineering & Remote Sensing, 2014, 80(10).
9. Sivagami K P, Jayanthi S K, Aranganayagi S, 'Detection of Image Edges using B^2MST', International Journal of Computational Intelligence and Informatics, 2016, 6(1), 42-52.
10. Sivagami K P, Jayanthi S K, Aranganayagi S, 'Monitoring Land Cover of Google Web Service Images through ECOC and ANFIS Classifiers,' International Journal of Computer Sciences and Engineering, 2017, 5(8), 9-16 (open access: https://doi.org/10.26438/ijcse/v5i8.916).
11. Stuart K. McFeeters, 'Using the Normalized Difference Water Index (NDWI) within a Geographic Information System to Detect Swimming Pools for Mosquito Abatement: A Practical Approach,' Remote sensing, 2013, 5, 3544-3561.

12. Tri Dev Acharya, In Tae Yang , Anoj Subedi, Dong Ha Lee, ' Change detection of lakes in Pokhara, Nepal using in Landsat data,' Proceedings 2017, 1(17), 1-6.
13. Wenbo Li, Zhiqiang Du, Feng Ling, Dongbo Zhou, Hailei Wang, Yuanmiao Gui, Bingyu Sun, Xiaoming Zhang , 'A comparison of land surface water mapping using the normalized difference water index from TM, ETM+ and ALI,' Remote sensing, 2013, 5, 5530-5549.
14. Yan Zhou, Jinwei Dong, Xiangming Xiao, Tong Xiao, Zhiqi Yang, Guosong Zhao, Zhenhua Zou, Yuanwei Qin, "Open Surface Water Mapping Algorithms: A comparison of water-related spectral indices and sensors," Water, 2017, 9(256), 1-16.